1521-0103/378/3/262–275$35.00
THE JOURNAL OF PHARMACOLOGY AND EXPERIMENTAL THERAPEUTICS

https://doi.org/10.1124/jpet.121.000590
J Pharmacol Exp Ther 378:262–275, September 2021

A Novel Selective PKR Inhibitor Restores Cognitive Deficits and Neurodegeneration in Alzheimer Disease Experimental Models[S]

Matilde Lopez-Grancha, Patrick Bernardelli, Nicolas Moindrot, Elisabeth Genet, Carine Vincent, Valerie Roudieres, Alain Krick, Jean-François Sabuco,[1] David Machnik, Delphine Ibghi, Laurent Pradier, and Veronique Taupin[2]

Neurodegeneration Cluster, Rare and Neurologic Disease Research TA (M.L.-G., N.M., E.G., C.V., V.R., D.I., L.P., V.T.), Integrated Drug Discovery (P.B., J.-F.S., D.M.), and DMPK (A.K.), Sanofi R&D, Chilly-Mazarin, France

Received March 03, 2021; accepted June 09, 2021

ABSTRACT

In Alzheimer disease (AD), the double-strand RNA-dependent kinase protein kinase R (PKR)/EIF2AK2 is activated in brain with increased phosphorylation of its substrate eukaryotic initiation factor 2α (eIF2α). AD risk-promoting factors, such as ApoE4 allele or the accumulation of neurotoxic amyloid-β oligomers (AβOs), have been associated with activation of PKR-dependent signaling. Here, we report the discovery of a novel potent and selective PKR inhibitor (SAR439883) and demonstrate its neuroprotective pharmacological activity in AD experimental models. In ApoE4 human replacement male mice, 1-week oral treatment with SAR439883 rescued short-term memory impairment in the spatial object recognition test and dose-dependently reduced learning and memory deficits in the Barnes maze test. Moreover, in AβO-injected male mice, a 2-week administration of SAR439883 in diet dose-dependently ameliorated the AβO-induced cognitive impairment in both Y-maze and Morris Water Maze, prevented loss of synaptic proteins, and reduced levels of the proinflammatory cytokine interleukin-1β. In both mouse models, these effects were associated with a dose-dependent inhibition of brain PKR activity as measured by both PKR occupancy and partial lowering of peIF2α levels. Our results provide evidence that selective pharmacological inhibition of PKR by a small selective molecule can rescue memory deficits and prevent neurodegeneration in animal models of AD-like pathology, suggesting that inhibition of PKR is a potential therapeutic approach for AD.

SIGNIFICANCE STATEMENT

This study reports the identification of a new small molecule potent and selective protein kinase R (PKR) inhibitor that can prevent cognitive deficits and neurodegeneration in Alzheimer disease (AD) experimental models, including a mouse model expressing the most prevalent AD genetic risk factor ApoE4. With high potency and selectivity, this PKR inhibitor represents a unique tool for investigating the physiological role of PKR and a starting point for developing new drug candidates for AD.

Introduction

The double-strand RNA-dependent kinase protein kinase R (PKR) (EIF2AK2) is one of the four kinases phosphorylating the α subunit of eukaryotic initiation factor 2α (eIF2α), thereby controlling protein translation in a global response known as the integrated stress response. The phosphorylation of eIF2α at Ser51 is tightly regulated by these four kinases, leading to inhibition of general protein translation while favoring translation of a limited subset of mRNAs, including the transcription factor activation transcription factor 4 (ATF4) (Lu et al., 2004, Vattem and Wek, 2004).

PKR is activated in neurodegenerative diseases, including Alzheimer disease (AD), as observed with accumulation of phosphorylated PKR (pPKR), its activated form, in degenerating neurons of human AD cortex and hippocampus compared with age-matched controls (Chang et al., 2002a; Peel and Bredesen, 2003; Onuki et al., 2004; Page et al., 2006; Paquet et al., 2012). Furthermore, pPKR is colocalized with phosphorylated eIF2α (peIF2α) in AD brain, and in cultured neurons, amyloid-β oligomers (AβOs) increase levels of peIF2α (Chang et al., 2002b; Morel et al., 2009; Mamada et al., 2015). In addition, levels of

This study received no external funding.

Matilde Lopez-Grancha, Patrick Bernardelli, Nicolas Moindrot, Elisabeth Genet, Carine Vincent, Valerie Roudieres, AIain Krick, David Machnik, Delphine Ibghi, Laurent Pradier, and Veronique Taupin are fully employed by Sanofi. Jean-François Sabuco was fully employed by Sanofi at the time studies were conducted and is now fully employed by Evotec. The authors declare that this manuscript is original, has not been published before, and is not currently being considered for publication elsewhere.

[1]*Current affiliation: Evotec ID, Marcy l'Etoile, France*
[2]*Current affiliation: Toxicology, Preclinical Safety, Global Operations France, Sanofi R&D, Montpellier, France*

http://doi.org/10.1124/jpet.121.000590.

[S] This article has supplemental material available at molpharm.aspetjournals.org.

ABBREVIATIONS: Aβ42, amyloid-β1-42; AD, Alzheimer disease; AβO, amyloid-β oligomer; BID, twice daily; eIF2a, eukaryotic initiation factor 2α; GCN2, general control nonderepressible 2; HEK, human embryonic kidney; IL-1β, interleukin-1β; KI, knock-in; KO, knockout; MWM, Morris Water Maze; ORT, object recognition test; PCR, polymerase chain reaction; peIF2α, phosphorylated eIF2α; PERK, PKR-like endoplasmic reticulum kinase; PKR, protein kinase R; pPERK, phosphorylated PERK; pPKR, phosphorylated PKR; RI, recognition index; PSD95, postsynaptic density protein 95; SNAP25, Synaptosomal-Associated Protein; WT, wild type.

pPKR are increased in CSF and in peripheral blood cells of patients with AD compared with healthy controls (Paccalin et al., 2006; Mouton-Liger, et al., 2012; Hugon et al., 2017). pPKR has therefore been proposed as potential biomarker for AD with high pPKR levels correlating with phosphorylated τ as well as predicting faster cognitive decline in newly diagnosed patients with AD (Dumurgier et al., 2013; Paquet et al., 2015).

ApoE4 allele, the highest genetic risk factor to develop AD (Kim et al., 2009) has also been associated with PKR activation in human PBMC (Peripheral Blood Mononuclear Cells) (Paccalin et al., 2006; Badia et al., 2013). PKR expression is increased in lymphocytes from young ApoE4 carriers and associated with subjective cognitive impairment (Badia et al., 2013). Consistent with these human data, humanized knock-in (KI) ApoE4 mice have increased peIF2α levels in hippocampus and cortex associated with cognitive deficits compared with control ApoE3-KI mice (Segev et al., 2013).

PKR/eIF2α pathway is involved in both memory formation/encoding and in response to neuronal and inflammatory stress, with ATF4 being critical for memory regulation (Chen et al., 2003; Costa-Mattioli et al., 2007, 2009; Buffington et al., 2014). In human ApoE4 carriers, ATF4 is overexpressed in postmortem brains (Baleriola et al., 2014; Segev et al., 2015). Conversely, enhanced long-term memory storage is observed in PKR-KO mice (Zhu et al., 2011) and in eIF2α-S51A mutant mice (Costa-Mattioli et al., 2007). PKR-KO mice were also shown to be resistant to intracerebroventricular injection of AβO. AβO-induced eIF2α inhibition and amnesic effect (Lourenco et al., 2013). In double-mutant 5xFAD/PKR-KO transgenic mice, spatial memory, synaptic alteration, and brain inflammation were ameliorated compared with 5xFAD mice (Tible et al., 2019).

Pharmacological inhibition or genetic inactivation of another eIF2α kinase, PERK (PKR-like endoplasmic reticulum kinase) , was shown to improve cognitive functions (Zhu et al., 2016), but PERK-KO mice develop pancreatic dysfunction that might represent serious liability for PERK inhibitors (Harding et al., 2001). Pharmacological inhibition of PKR with the small molecule C16 was also shown to enhance cognitive performance in wild-type mice (Ingrand et al., 2007; Stern et al., 2013; Zhu et al., 2011) and to reverse deficits in ApoE4-KI (Segev et al., 2015), but C16 lacks potency and selectivity versus other eIF2AKs and other kinases (Chen et al., 2008). Our first-generation PKR inhibitor was previously demonstrated to provide neuroprotection in a short-term model of thiamine deficiency (Mouton-Liger et al., 2015).

We now report on a novel isoindolinone, SAR439883, with improved selectivity as well as drug-like properties and demonstrate its protective/restorative effects on cognitive deficits and on synaptic loss in two AD-related animal models. SAR439883 is a potent and orally bioavailable PKR inhibitor highly selective versus other eIF2AKs and kinases. Oral administration of SAR439883 restores cognitive function in ApoE4-KI mice and protects from cognitive deficits and neurodegeneration markers in AβO intracerebroventricularly injected mice. Our results suggest that PKR-selective inhibition represents a potential therapeutic treatment of AD.

Materials and Methods

Synthesis of SAR439883

SAR439883 has been synthetized by the medicinal chemistry department of Sanofi R&D after medicinal chemistry optimization from an isoindolinone chemical series (see structure in Fig. 1A and chemical synthesis in Supplemental Material provided online). SAR439883 was tested through a high-throughput screening based on a biochemical assay measuring the inhibitory effect of compound on human PKR-mediated phosphorylation of its substrate eIF2α.

Biochemical Assay for Kinase Activity

HTRF technology (Homogeneous Time Resolved Fluorescence, Cis-Bio) was used to determine compound activity on PKR.

First, PKR or PERK or GCN 2, his-tagged eIF2α (Sanofi) as substrate, ds polyIC and ATP (Sigma) as cosubstrates, and $MgCl_2$ (Sigma) were mixed for allowing phosphorylation of eIF2α. Then, the reaction was stopped by addition of the HTRF reagents (Cisbio) diluted in HTRF buffer containing EDTA. The phosphorylated form of eIF2α was titrated by the HTRF reagents. The anti–his-XL bound to the his-tag of eIF2α. The antiphospho-eIF2α-cryptate bound to peIF2α. A signal at 665 nM was generated by energy transfer from the cryptate (emission at 620 nm after laser excitation) to the XL when the two fluorophores were held in proximity. The signal at 665 nm is thus proportional to the quantity of peIF2α produced during the enzymatic reaction. Signals detected by HTRF were the fluorescence intensity at both 665 nm and 620 nm. The HTRF signal corresponded to the ratio em665 nm/em620 nm. Background signal corresponded to the ratio from control samples in which the enzyme activity was fully inhibited by an excess of EDTA or was absent. Total signal corresponded to the ratio from control samples in which enzyme was incubated with eIF2α substrate and cosubstrates (ATP, ds polyIC) in the absence of inhibitor compound.

Activity on Cdk9 was measured by binding (IMAP technology, Molecular Devices) revealed by fluorescent polarization.

For PKR compound, the concentration-inhibition curve and IC50 value (concentration giving 50% inhibition of enzymatic activity) are determined by nonlinear regression analysis by using Speed V2.0 software (developed by Sanofi).

Cellular Assay for PKR

The assay for PKR activity was based on the use of an inducible HEK -293-FlpIn-TRex cell line expressing either human or murine PKR. Cells were plated in 96-well plates (Greiner, µclear Poly-D-lysine) at the density of 10,000 cells/well in Dulbecco's modified Eagle's medium (Gibco Invitrogen) +10% FCS (Fetal Calf Serum, Gibco Invitrogen) and incubated at 5% CO_2, 37°C. After doxycycline induction (50 mg/ml, 16 hours), the compound was added and incubated for 4 hours with the cells that overexpress the human recombinant PKR. At the end of the incubation, the cells were fixed with formaldehyde 4% and permeabilized with PBS/0.2% Triton X-100 for immunostaining with both rabbit anti-peIF2α (Biosource) and goat anti-eIF2α (Santacruz) antibodies. PKR activity was determined by direct measurement of the phosphorylation of the native substrate eIF2α. PeIF2α level was determined by image analysis with InCell Analyzer 2200 (GE Healthcare). The intensity of the fluorescence signal at Ex480nm/Em535 is proportional to the quantity of peIF2α in cells. The intensity of the signal at Ex595/Em620 is proportional to the quantity of total eIF2α. Cell number was measured by counting the nuclei after DAPI (4',6-diamidino-2-phénylindole) staining. The maximal response corresponds to the percentage of cells in the wells in which the recombinant PKR was maximally induced with doxycycline and without compound.

Cellular assay for PERK: Activity on phosphorylated PERK (pPERK) was evaluated by measuring the autophosphorylation of PERK in A549 cell line in which pPERK expression was induced by treatment with thapsigargin.

Cellular assay for GCN2: Activity on phospho-GCN2 (pGCN2) was evaluated by measuring the autophosphorylation of GCN2 in A549 cell line in which pGCN2 expression was induced by treatment with L-tryptophanol.

For the tested compound, the concentration-inhibition curve and IC_{50} value were determined by nonlinear regression analysis by using Speed V2.0 software (developed by Sanofi).

Primary Neuronal Cultures

Primary neuronal cultures were prepared from brain of 16-day-old mouse (OF1, Charles River Laboratories, France) embryos by dissecting and then dissociating cerebral cortices. Cells were plated in Dulbecco's modified Eagle's medium supplemented with N2 and B27 at a cell density of 4 × 105 cells/ml in poly-D-lysine–coated wells of 96-well culture microplate. After 6 days in vitro, neurons were incubated with AβO42 (5 μM) for 48 hours. Cell treatment with drug-free medium but supplemented with the corresponding DMSO concentration (i.e., 0.1%, same as for AβO treatment) was run in parallel to test substance.

Quantification of Caspase 3/7 Enzymatic Activity. After experimental treatment, caspase-Glo 3/7 Assay kit solution (Promega Corporation USA, G7790) was mixed to each well and then incubated for 4 hours at room temperature. After incubation, the fluorescence of each sample was quantified using a Spectramax Gemini plate reader. The measurement of fluorescence intensity is proportional to caspase 3/7 enzymatic activity.

Quantification of peIF2α Levels in Primary Neuronal Cultures

Phosphorylated eIF2α levels were determined by Western blot analysis of the ratio between peIF2α and total eIF2α with the following antibodies: anti–phosphoSer51 eIF2α antibody (3398S, D9G8) and anti-total eIF2α antibody (9722S) from Cell Signaling Technology. Briefly, aliquots of cell extracts (20 μg of protein) were separated by 4%–12% gradients SDS-PAGE and transferred onto polyvinylidene fluoride membranes (NP0336, InvitroGen). The membranes were probed with the following antibodies: rabbit anti-eIF2α and rabbit anti-peIF2α from Cell Signaling; horseradish peroxidase–conjugated rabbit or mouse secondary antibodies were used (Promega), and after extensive washing, the immunoreactive bands were detected by enhanced chemiluminescence (ECL Select Amersham RPN2235). Image acquisition and analysis was performed with the Amersham imager S600 and the Multi Gauge software.

Animals

Experiments were performed in our American Association for Accreditation of Laboratory Animal Care –accredited facility or at SynAging (Contract Research Organization, France) in full compliance with standards for the care and use of laboratory animals, according to French and European Community (Directive 2010 /63/EU) legislation. All procedures were approved by the local Animal Ethic Committees and the French Ministry for Research. All animal experiments were designed with a commitment to refinement, reduction, and replacement, minimizing the number of mice and suffering via emphasis on human end points while using biostatistical advice for optimization of mouse number.

To reduce the variability introduced by sex factors, such as the hormonal fluctuation that occurs during the estrous cycle (Meziane et al., 2007) and based on cognitive and metabolic differences between male and female ApoE3 and ApoE4-KI mice obtained in our laboratories (unpublished data), only male mice were used in these studies.

Animals (housed 4 to 5 per cage) were kept in a pathogen-free facility at a constant temperature of 22 ± 2°C and humidity (50 ± 10%) on a 12-hour light/dark cycle (lights on at 7 AM) with ad libitum access to food and water except during the tests. All tests were conducted during the light phase at roughly the same time each day to minimize variability in performance due to time of day (between 9 AM and 4 PM) unless otherwise specified. For the behavioral tests, the mice were brought to the experimental room for at least 30 minutes acclimation prior to testing. The animals were randomized to the treatment groups according to their body weight, the timing of test sessions, and the different enclosures used in the spatial recognition test. For each experiment, the mice were assigned identification numbers so that the experimenters were blinded to the treatment conditions (genotype, treatment, AβO or vehicle intracerebroventricular stereotaxic injection) as well as during cognitive testing and scoring.

Fifteen homozygous human ApoE3 and 79 male homozygous human ApoE4 targeted replacement mice (catalog numbers 001548 and 001549, Taconic Farm) were used for evaluating the effect of our PKR inhibitor on short- and long-term memory. ApoE4 human targeted replacement mice (ApoE4-KI) express the human ApoE4 isoform under the control of endogenous murine ApoE regulatory sequences (Sullivan et al., 1997) while mouse ApoE has been deleted. C57B6/J mice obtained from Charles River were also used. For the Barnes maze test, PKR inhibitor SAR439883 (base form) was given BID by gavage at 10 and 30 mg/kg of body weight in 0.6% methylcellulose/0.5% Tween-80 for 7 days (first administration in the mornings 1 hour before the training and the second one 6 hours later). On day 8, mice received the last administration 1 hour before the probe test and were sacrificed immediately after. For spatial object recognition, 5.5-month-old mice were treated for 7 days with vehicle or SAR439883 incorporated in the diet (Ssniff Spezialdiäten GmbH) at two concentrations (0.1% and 0.3%). Considering the exposure in the plasma after a single oral administration (unpublished data), 0.1% SAR439883 in the diet was calculated to be bioequivalent to a 10-mg/kg single oral dose. Testing occurred on day 7.

AβO Intracerebroventricular Injection Model

Amyloid-β1-42 (Aβ42) was obtained from Bachem (H1368, batch number 1052301). The stable Aβ42 oligomers were prepared according to SynAging protocol (Garcia et al., 2010). The oligomeric preparation contains a mixture of stable trimers and tetramers of Aβ42 as well as monomeric forms of the peptides. Oligomer preparation was previously characterized in terms of oligomer composition and in vitro neurotoxicity by SynAging and called AβO. Global experimental design is illustrated in Fig. 4A. Briefly, 73 C57BI6/J male (3-month-old) mice were fed with the diet, either control diet (vehicle Ssniff Spezialdiäten GmbH) or diet containing the PKR inhibitor at three different concentrations (0.03%, 0.1%, 0.3%), 3 days before the induction of the disease. At day 0, mice received under anesthesia a single unilateral intracerebroventricular injection of vehicle or AβO (50 pmol/1 μl) into the right lateral ventricle.

Four days after disease induction, spatial working memory was assessed using the Y-maze test. From days +3 to days +14, learning capacities and long-term memory were investigated in the MWM assay. Animals were sacrificed at day +15, and tissues were prepared for further ex vivo analyses. During the entire protocol, animals were weighted every other day from day −10 to day +15.

Behavioral Tests

Y-Maze and Morris Water Maze. Immediate spatial working memory performance was assessed by recording spontaneous alternation behavior in a Y-maze. Spontaneous alternation is a natural tendency of the animals of numerous species, including rodents, to alternate their response when facing identical and repeated choices. Its rating in a Y-maze allows the evaluation of spatial orientation capabilities (Hughes, 2004). Animal performances in mazes are related to the integrity of hippocampus and spatial memory function (Roberts et al., 1962; Means et al., 1971). The maze is made of opaque Plexiglas, and each of the three arms is 40 cm long, 16 cm high, 9 cm wide, and positioned at equal angles. The apparatus was placed in a homogeneously lit test room to obtain 15 lux in all arms as well as in the central zone. Mice were placed in the middle of one arm and allowed to explore the maze freely during 5-minute sessions. The series of arm entries were video recorded (Smart v3.0 software, Bioseb). An arm entry was considered complete when the hind paws of the mouse were completely placed in the arm. Alternation was defined as successive entries into the three arms on overlapping triplet sets. The percentage alternation was calculated as the ratio of actual (total

alternations) to possible alternations (defined as the number of arm entries minus two) multiplied by 100. Locomotor activity was also recorded and evaluated by monitoring average speed and total distance. Mice were discarded if they did not perform the minimum of 12 arm entries or if they exhibited aberrant behaviors (e.g., mice followed the wall or presented anxious behaviors).

Spatial learning capabilities and long-term memory were further investigated using the MWM as described previously (Garcia et al., 2010). The experimental apparatus consisted of a circular white opaque plastic water tank (diameter, 90 cm; height, 50 cm) containing water (21°C) to a depth of 25 cm. A white artificial colorant (Lytron) was spread over the water surface to camouflage the escape platform (5 cm × 5 cm) made of white plastic and covered with a wire mesh to ensure a firm grip. The pool was placed in a test room homogeneously lit at 100 lux. The swimming paths, swimming distance, swimming speed, and thigmotaxis were recorded using a video tracking system (Smart v3.0 software, Bioseb.) The MWM assay consists of three different steps described as follows: ***Habituation (visible platform, no visual cues)***—navigation to a visible platform was carried out before place navigation to evaluate visual and motor abilities of mice. Mice were submitted to four trials (two trials in the morning and two trials in the afternoon) of 60 seconds each per day during 2 consecutive days with an intertrial interval of at least 1 hour. Once mice found the platform, they were left alone on the platform for an additional time of 30 seconds. There were no additional maze cues in the room. The platform position and starting points were randomly distributed over all four quadrants of the pool. Mice that failed to find the platform after 60 seconds were guided to its location and placed on it for 30 seconds. After removal from the pool, mice were manually dried with a terry-cloth towel and placed in their home cage. Next, ***memory-acquisition*** (learning trials with hidden platform, visual cu*es)* was performed during 5 consecutive days. Several prominent visual cues on the wall near the rim of the pool were added. The hidden platform was submerged 1 cm below the water surface and placed at the midpoint of one quadrant. Mice were submitted to four trials of 60 seconds per day with an intertrial interval of at least 1 hour. The mice were allowed to swim freely for 60 seconds, left alone for an additional 30 seconds on the hidden platform and then returned to the home cage during the intertrial interval. Start positions (set at the border between quadrants) were randomly selected for each animal. In each trial, the time required to escape onto the hidden platform was recorded. Mice failing to find the platform within 60 seconds were placed on the platform for 30 seconds before returning to their home cage. ***Memory-retention test (probe trial)*** was performed 3 days after the last training session. The platform was removed, and each animal was allowed a free 60-second swim. During the probe trial, the time spent in the target quadrant, the number of crossings over the original platform point, and the time required for the first crossing over were registered and monitored by video tracking. In habituation, the mean latency and swim speed for the second day were calculated for each mouse. Mice with two standard deviations above the group mean were excluded, as this may be indicative of motor or visual impairments. Mice exhibiting aberrant behavior, such as cork-screw swimming or floating most of the time, were also discarded.

Spatial Object Recognition Test. This test relies on rodents' natural proactivity for exploring novelty (Ennaceur and Delacour, 1988) and was adapted for use in mice and performed as previously described (Delay-Goyet et al., 2016). Accordingly, two weeks before the start of the study, mice were housed individually in an enriched environment. On days 1 and 2, mice were allowed to become familiar with the experimental environment twice a day for 10 minutes. It consisted of four PVC (polyvinyl chloride) enclosures (59 × 59 × 30 cm height) with four black walls, a white floor, and a video camera positioned 160 cm above the bench. The arenas were uniformly lit (30 lux). On day 3, mice were placed in the test enclosure in the presence of two identical objects placed in diagonal. Time spent exploring each object during the 10 minutes was recorded (exploration was defined as the animal having its head within 2 cm of the object while looking at, sniffing, or touching it). After a forgetting interval of 1 hour, mice were placed back in the enclosure (recall session) for 10 minutes with one of the objects (A) in the same location as before (familiar) and the other object (B) in a novel location. Ambient cues in the room served as place references. Time spent exploring the familiar and novel location (in seconds) was recorded. A recognition index was calculated as follows: 100 × time for object B/(time for object A + time for object B) for the 10 minutes of the recall phase. For a short-term forgetting delay, during the recall session, normal mice spent more time exploring the novel location of the object compared with the familiar one. That reflects a remembering of the familiar location.

The different objects were counterbalanced and were used equally as old and novel objects. Objects were cleaned with 70% ethanol between phases to eliminate odor cues. During both training and testing, mice should explore at least 2 seconds each object. First exploration should be done before 6 minutes, otherwise the mice will be excluded. $N = 12$ was the sample size calculated to detect an absolute difference of at least 10% with 90% or 75% power when the variability is median and high, respectively.

Barnes Test. The Barnes maze task was employed to test spatial memory as described previously (Barnes, 1979). It consisted of a white circular polyethylene platform 92 cm in diameter with 20 holes measuring 5 cm in diameter evenly spaced around the perimeter (2 cm from the edge) of an elevated (70 cm above the floor) maze. One of the holes led to a black Plexiglas escape box (5 × 5 × 11 cm) filled with sawdust. The maze was illuminated by overhead fluorescent white room lighting (400 lux) and surrounded by white walls, which contained spatial cues (posters with different figures). Mice were trained to locate the escape box hidden underneath 1 of 20 holes. The location of the escape hole remained constant throughout the training sessions. To familiarize mice with the maze and the existence of the escape hole, they were subjected to a pretraining session (identical to the training sessions). At the beginning of the trial to prevent orientation to the target, the mouse was placed in the middle of the maze under a start chamber (a cylinder black box, 12 cm in diameter), and a buzzer (80 dB) was turned on. After 10 seconds, the chamber was lifted, and the mouse was gently guided by the experimenter to the escape hole, the buzzer was turned off, and the mouse remained in the box for 60 seconds. During the acquisition trials, the animals were allowed to freely explore the maze and used the distal cues to localize and to enter the escape hole. Mice were given four training trials per day with a 15-minute intertrial interval over 5 days. Each trial took 3 minutes long or ended when the mouse entered the escape box, whatever came first. If a mouse did not enter the escape hole within 3 minutes, it was gently pulled by the experimenter to the escape box and allowed to stay there for 60 seconds. A 70% ethanol solution was used to wipe clean the platform after every trial and the escape box after each session. Seventy-two hours later, mice were given a 90-second probe trial transfer test without the escape hole. During this trial all the holes were closed and there was no escape box. Trials were recorded using a camera mounted above the maze, and animals' movements were tracked and analyzed using a video tracking system (Viewpoint). Performance was assessed by latency to reach the virtual escape hole and time spent in the escape hole zone. Mice not moving during the 90 seconds of the probe test were excluded from the analysis. The sample size $N = 12$ by group of ApoE4 enables the showing of a difference at 72 hours of at least 50% for the parameter time spent in the target quadrant with a power of 82%.

Quantification of SAR439883 in Blood and Brain Tissues

At the completion of the experiments, mice were anesthetized using a mixture of 100 mg ketamine plus 10 mg/kg xylazine, and blood samples were collected by cardiac puncture into Sarstedt Lithium-Heparin gel tubes. After centrifugation (1500–2000g for 10 minutes at 4°C), plasma samples were frozen in microtubes and stored at −80°C. Then, brains were removed. Hippocampi, cortex, pons, and cerebellum were collected and stored at −80°C until they were used for

biochemical, RNA, or pharmacokinetics (PK) analyses. For the quantification of SAR439883 levels, after the addition of the precipitant solution (acetonitrile), SAR439883 was quantified in both plasma and pons/cerebellum samples by liquid chromatography–mass spectrometry/mass spectrometry.

Preparation of Hippocampal and Brain Cortical Homogenates

Hippocampi or brain cortices were homogenized in cold RIPA buffer (Cell Signaling, 9806) containing an anti-protease cocktail (Roche, 05056489001), 1 mM PMSF (phenylmethylsulfonyl fluoride) , and 1 mM sodium orthovanadate added freshly just before use. Samples were vortexed, kept on ice for 10 minutes, and exposed to three freeze-thaw cycles (liquid nitrogen). Lysates were centrifuged at 800g for 15 minutes at 4°C. The supernatant was dispensed into aliquots and stored at −80°C for later analysis. Total protein content was assessed using the BCA assay. Data were recorded using a FLUOSTAR-Omega plate reader (BMG-LABTECH) and expressed as milligram protein per milliliter.

KiNativ Binding Selectivity Assay

Target occupancy in-cell lysates (PC3 cell line) or in brain homogenates after in vivo treatment with SAR439883 was performed using KiNativ platform to quantitatively profile responses of our PKR inhibitor against PKR and all kinases detectable in brain extract. KiNativ is based on biotinylated acyl phosphates of ATP and ADP that irreversibly react with protein kinases on conserved lysine residues in the ATP-binding pocket. The ActivX unique chemical probes combined with quantitative mass spectrometry of pulled-down proteins yield relative quantification of kinases detectable in sample. Presence of a catalytic site kinase inhibitor in a sample prevents ActivX probe binding and can be differentially quantified compared with samples without inhibitor. For each kinase detected, the occupancy by the inhibitor is reported as percentage versus sample without inhibitor as described by KiNativ. PKR was detectable in brain samples as well as over 200 other ATP/ADP binding kinases.

Real-Time Polymerase Chain Reaction on Mouse Brain Tissues

Mouse brain cortical tissues were homogenized using Precellys. Total RNA extraction from the hippocampus was performed using the RNAeasy Tissue mini kit (QIAGEN) according to the manufacturer's recommendations. Reverse transcription was performed using High-Capacity cDNA Reverse Transcription kit (Applied Biosystems). Real-time PCR was performed with TaqMan universal PCR master mix (Applied Biosystems) using the cDNA and gene-specific TaqMan reactions (Applied Biosystems). Real-time PCRs were performed in triplicate using the thermocycler Quant Studio3 (Applied Biosystems) under the following conditions: 50°C for 2 minutes, 95°C for 10 minutes, and 40 cycles of 95°C for 15 seconds and 60°C for 1 minute. Threshold cycle values of the general ATF4 (Mm00515325_g1) were normalized to the threshold cycle values of the mouse GAPDH (Mm99999915g-1) and hypoxanthine phosphoribosyl transferase (Mm0154599m-1).

Quantification of peIF2α Levels in Brain Tissue Samples

peIF2α levels were analyzed by measuring the ratio between peIF2α and total eIF2α using Simple Western Assay (Sally Sue, ProteinSimple Technology) designed to run an automated Western blot–like workflow and the following antibodies: anti–phosphoSer51 eIF2α antibody (3398S, D9G8) and anti-total eIF2α antibody (9722S) from Cell Signaling Technology. Target proteins were immunoprobed and detected by chemiluminescence and automatically detected and analyzed.

Synaptic and Neuroinflammation Markers

AβO-injected animals were sacrificed at day 15, and brain tissues were sampled for further ex vivo analyses. Brain levels of PSD95 (postsynaptic density protein 95) , SNAP (Synaptosomal-Associated Protein) 25, synaptophysin, and IL-1β were assessed by ELISA in hippocampal lysates using commercially available kits, using a FLUOSTAR-Omega plate reader (BMG-LABTECH), and according to manufacturer's recommendations (Cloud-Clone Corp.)

Statistical Analysis

Everstat V6 based on SAS 9.2 software was used for statistical analysis. Differences between control and treated groups were analyzed using one-way ANOVA on raw data followed by a Dunnett's test (biochemical data; Y-maze) or repeated two-way ANOVA followed by a post hoc Student test for each group (MMW). The significance level was taken to 5%. GraphPad/Prism software was used for figures. In spatial object recognition test, ApoE3-KI and ApoE4-KI vehicle groups were compared by performing a two-way ANOVA with factors week and group followed by a Dunnett's test for treated mice. In the Barnes test, because of censored values for the parameter "latency to find the escape hole" in the acquisition phase, a time-to-event analysis was performed for data obtained in the Barnes test. A Gehan test was used for comparing ApoE4-KI and C57B6/J vehicle groups. Gehan tests were adjusted for multiplicity by Bonferroni-Holm correction to compare ApoE4-KI–treated mice. For the "latency to the escape hole" in probe trial test, a one-way ANOVA followed by a Dunnett's test comparing ApoE-KI–treated mice versus ApoE4-KI vehicle mice.

Results

In Vitro, SAR439883 Is a Soluble, Potent, and Selective PKR Inhibitor. SAR439883 has been developed by a medicinal chemistry optimization (see structure in Fig. 1A) starting from a chemical series discovered in a high-throughput screening using a biochemical assay to measure the inhibitory effect of compound on human PKR-mediated phosphorylation of its substrate eIF2α. In this assay, SAR439883 was demonstrated to be a potent PKR inhibitor with an IC_{50} of 30 nM (Table 1). In inducible murine and human PKR-expressing HEK cell lines, SAR439883 potently inhibited eIF2α phosphorylation with IC_{50} of 0.69 μM and 0.68 μM, respectively (Fig. 1B). In biochemical assays, it displayed some activity on the other EIF2AK, GCN2 (62nM) but not PERK (1260nM) (Table 1). Otherwise SAR439883 had a particularly good kinase selectivity with only weak activity on cyclin-dependent kinase 9 (IC_{50} 964 nM) and good selectivity in extensive panels of receptors and enzymes (304 kinases and 148 receptors/ion channels tested in Eurofins) (unpublished data; Table 1).

When measuring autophosphorylation, SAR439883 was 30-fold more selective for PKR versus GCN (i.e., IC_{50} of 179nM for pPKR and 6.3 μM for pGCN2) and showed greater than 500-fold selectivity versus other eiF2AKs PERK and HRI (Heme-regulated eIF2α kinase) (unpublished data; Table 1). ActivX/KiNativ profiling (that measured occupancy of the ATP-binding site of all detectable kinases in a sample) confirmed activity and increased selectivity of SAR439883 particularly versus GCN2 both in cells and in vivo at C_{max} of brain exposure (Table 2; Supplemental Table 1).

In isolated neuronal cultures, we demonstrated both an elevation of peIF2α induced by AβO and its reversion by

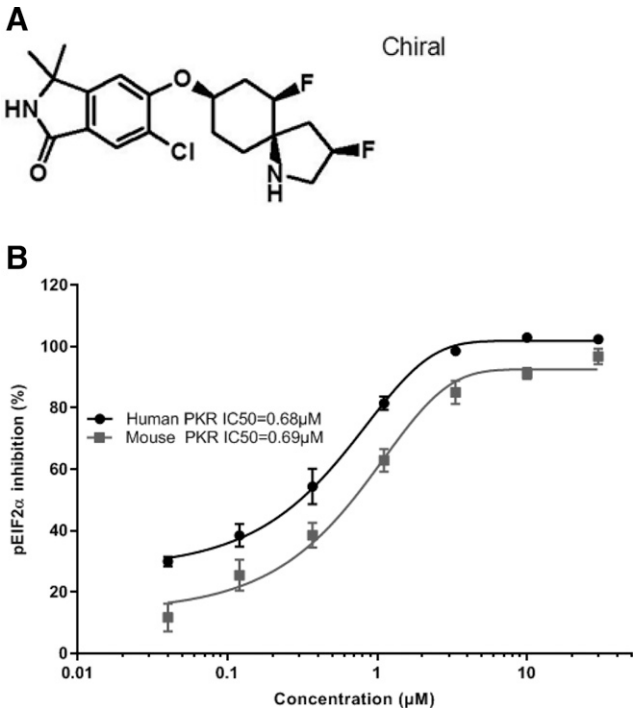

Fig. 1. SAR439883 compound. (A) Chemical structure of SAR439883: 6-chloro-5-[[(3*R*,5*R*,6*R*,8*R*)-3,6-difluoro-1-azaspiro[4.5]decan-8-yl]oxy]-3,3-dimethyl-isoindolin-1-one - C19H23CIF2N2O2. (B) Inhibition profile of phospho-eIF2α levels by SAR439883 in murine and in human PKR-inducible HEK cells. Mouse or human PKR-expressing HEK cells were induced overnight with doxycycline then treated with SAR439883 for 4 hours. Data are presented as mean ± S.D. from six replicates per tested concentration and expressed as % peIF2α inhibition of control. Calculation of the relative IC_{50} for both human and mouse PKR determined using Speed V2.0 software .

SAR439883 at 3 μM, which correlates with its protective effect against Aβ*O* neurotoxicity as measured by caspase-3/7 enzymatic activity (Supplemental Fig. 1; Supplemental Table 3).

Oral bioavailability and brain penetration after oral gavage (30 mg/kg) were documented in wild-type (WT) mice under standard procedure ($t_{1/2}$ = 2.6 hours, unbound fraction = 10%, C_{max} brain = 6.6 μM, brain-to-plasma ratio = 0.34; unpublished data Supplemental Fig. 2). In vivo activity after oral administration was confirmed with inhibition of hippocampal peIF2a levels by −51% and −61% at tmax (the time taken to reach the maximum concentration) at doses of 30 and 100 mg/kg, respectively (Supplemental Fig. 3). For subchronic administration in diet and to determine the optimal time point for analyzing PKR target, engagement in brain, plasma, and brain concentration of SAR439883 was analyzed in C57BL6/J mice (WT) at different timepoints (7 PM, 8 PM, 2 AM, 8 AM, 2 PM) between day 7 and day 8 of treatment, and the corresponding brain peIF2α decrease was evaluated for both 0.1% and 0.3% doses (Supplemental Table 2). As mice are known to feed more during the night than daytime, we focused the assessments during the night period to determine the maximum SAR439883 concentration. A dose-dependent increase in blood and brain total concentrations was observed together with stronger inhibition of brain peIF2α levels. Maximum inhibition of peIF2α (−53%) was obtained at 2 AM corresponding to highest brain compound exposure in WT mice.

SAR439883 Subchronic Treatment Normalizes PKR Overactivation and Cognitive Deficits in ApoE4-KI Mouse. PKR has been shown to be overactivated and eIF2α phosphorylation increased in brain of ApoE4-KI compared with ApoE3-KI mice (Segev et al., 2013, 2015). We confirmed that levels of brain eIF2α phosphorylation were significantly increased in ApoE4-KI mice carrying two alleles of the human E4 compared with ApoE3 counterparts (i.e., +27%, $P < 0.0001$; Fig. 2A). Likewise, the downstream marker of eIF2α pathway ATF4 was upregulated in ApoE4 versus ApoE3-KI animals ($P < 0.0001$, Fig. 2B).

The optimal experimental conditions [i.e., a 7-day treatment in diet (0.1% and 0.3%) with SAR439883 and sampling at 2 AM] were applied to ApoE4-KI mice. PKR inhibitor decreased brain peIF2α levels in a dose-dependent manner (−34% and −43%, at 0.1% and 0.3% in diet, respectively) trending to be lower than levels for ApoE3-KI control mice (Fig. 2A). Consistently, ATF4 mRNA expression was reversed by 52% and 61% after a 0.1 and 0.3% SAR439883 treatment, respectively, compared with vehicle in ApoE4-KI mouse (Fig. 2B).

Additional markers linked to ATF4/eIF2α downstream pathway, CHOP (CCAAT/enhancer binding protein (C/EBP) homologous protein) , EGR1 (early growth response 1 factor), Ophn1 (Oligophrenin-1), and GADD34 were investigated at the mRNA levels but were not significantly modulated by either the ApoE4 genotype or after PKR inhibitor treatment (unpublished data).

Remarkably, the kinase profiling performed in ex vivo brain samples using the KiNativ/ActivX technology revealed a strong and selective binding of SAR439883 compound to PKR (81% and 90% target occupancy for the doses of 0.1% and 0.3% in diet, respectively; Table 2) and high selectivity among a panel of more than 200 kinases detected. In association to the PKR engagement, the 7-day treatment with SAR439883 reversed deficits in short-term memory displayed by ApoE4-KI mice. As shown in Fig. 2C, the recognition index (50.9 ± 1.8%) displayed by vehicle ApoE4-KI mice was significantly lower $P < 0.0001$ than for vehicle ApoE3-KI mice (65.7 ± 2.1%), confirming the cognitive deficits associated to the E4 allele previously reported (Salomon-Zimri et al., 2014). In animals treated with the PKR inhibitor, mean recognition indexes were increased to 60.2 ± 2.4% ($P = 0.0114$) and 61.6 ± 2.0% ($P = 0.0035$) in the 0.1% and 0.3% SAR439883 dose groups, respectively (Fig. 2C). Both doses partially reversed the deficit. Two ApoE3-KI mice (vehicle) and one ApoE4-KI mouse (vehicle) were excluded from the analysis because of a lack of exploration, as specified in the protocol.

Learning and long-term memory improvements were also documented in a separate study using the Barnes test (Fig. 3A). Here, SAR439883 (10–30 mg/kg BID per os) was administered from the beginning of the training. Figure 3B shows the latency to find the escape hole during the acquisition learning. ApoE4-KI mice show a strong deficit in learning process ($P < 0.0001$ at days 3, 4, and 5) compared with C57B6J mice. ApoE4-KI mice deficits were partly reversed by SAR439883 treatment at 30 mg/kg ($P < 0.001$) but not with the lower dose. Seventy-two hours after the last training trial, all the holes were closed, and animals were tested in a single 90-second probe trial to assess long-term spatial memory. ApoE4-KI mice displayed a longer latency to the escape hole ($P = 0.0017$, Fig. 3C) and spent less time in the target hole

TABLE 1
In vitro profile of SAR439883 compound
Data are expressed as mean ± S.D. from 1 (Cellular GCN2) to five independent experiments.

Activity	Kinase	SAR439883 IC_{50}
		nM
Biochemical (human)	PKR (peIF2α, ATP 40 μM)	30 ±**3**
	PERK (ATP 2 μM)	1260 ± 121
	GCN2 (ATP 40 μM)	62 ± 4
	Cyclin-dependent kinase 9 (ATP 10 μM)	64 ± 103
Cellular (human)	PKR (pPKR)	179 ± 53
	PKR (peIF2α)	678 ± 149
	PERK (pPERK)	inactive up to 30,000
	GCN2 (pGCN2)	6300

quadrant ($P = 0.0049$; Fig. 3D) than C57BL6/J vehicle mice. These long-term memory deficits in ApoE4-KI mice were reversed with the higher dose of SAR439883 (30 mg/kg; $P = 0.0406$ and $P = 0.0004$ for the latency to the escape hole and time spent in the escape hole quadrant, respectively) (Fig. 3, C and D). There only was a non–statistically significant trend at the lower dose.

SAR439883 Prevents Acute AβO-Induced Cognitive Impairment. It has been previously reported that intracerebroventricular injection of soluble Aβ oligomers (AβOs) triggers inflammatory response and cellular stress leading to direct damage to synapses (Ferreira and Klein, 2011; Ferreira et al., 2015; Viola and Klein, 2015). AβOs have been used as neurotoxins in experimental mouse model (Balducci and Forloni, 2014) and triggered PKR kinase activation, promoting synapse and memory impairments (Paquet et al., 2012; Bomfim et al., 2012; Lourenco et al., 2013; Ma et al., 2013).

Therefore, we assessed the effect of our PKR inhibitor SAR439883 on the AβO-induced cognitive deficit, inflammation, and synapse loss. The full experimental design over 15 days is described in Fig. 4A. A group of animals receiving humanin was used as positive treatment control, as it has been shown to reverse inflammation and neurodegeneration in this model (Yuan et al., 2016). The spatial working memory was investigated using the Y-maze on day 4 post–AβO injection. Fifteen mice were excluded from the analysis as specified in the protocol (fewer than 12 arm entries or abnormal behavior). The AβO-injected mice deficit in spatial working memory (16% decrease in alternation behavior, $P = 0.0019$) compared with control mice was fully reversed by humanin ($P < 0.05$) or by the 0.3% SAR439883 diet ($P < 0.05$; Fig. 4B). Total distance was also analyzed and showed no difference among all the experimental groups ($P = 0.1148$), indicating that changes in alternation behavior were not due to generalized exploratory or locomotor effects. The wide dispersion at the two lower doses prevented from reaching statistical significance but trended for improvement.

Spatial learning and long-term memory were further explored in the MWM task (Fig. 4, C and D; Supplemental Fig. 4). Performance in the MWM is influenced by sensorimotor function and motivation, and these parameters were assessed using a visual cue test. Escape latency during the visual cue test was decreased from day 1 to day 2 in all the groups, whereas the swim speed remained unchanged over the sessions. On learning phase, no significant differences were observed in escape latency between vehicle mice and every group globally and at each day (unpublished data).

To assess spatial long-term memory, a probe trial was administered 72 hours after the last learning session. As expected AβO intracerebroventricular injection adversely affected performance in the probe test with an increased escape latency ($P = 0.0338$) and a decreased number of target crossings ($P = 0.001$) compared with vehicle animals. This memory impairment was completely prevented by humanin

TABLE 2
Effect of a 7-day treatment with SAR439883 on PKR activation and cognition in ApoE4 mouse
Data are expressed as mean ± S.E.M.

	Cognition	PKR Engagement	Compound Conc.				
SAR439883	ORT (Recognition Index)[a]	peIF2α Inhibition[b]	ATF4 Reversion[b]	Occupancy % (ActivX/KiNativ)[c]	Brain[d]	Plasma[d]	
				PKR	GCN2		
% in diet	*Δ points*	*%*	*%*			*μM*	*μM*
0.1%	9.3 ± 0.4	34.3 ± 1.8	52.1 ± 0.7	81.2 ± 1.4	None	1.5 ± 0.2	6.6 ± 0.7
	$P = 0.0114$	$P < 0.0001$	$P < 0.0001$				
0.3%	10.7 ± 0.3	43.4 ± 2.8	61.0 ± 0.9	90.2 ± 1.8	None	3.3 ± 0.2	15.2 ± 2.2
	$P = 0.0035$	$P = 0.0001$	$P < 0.0001$				

[a]Δ points: Δ of Recognition Index (ORT).
[b]Inhibition of PKR pathway (peIF2α and ATF4 brain expression) by SAR439883.
[c]PKR selectivity measured in ex vivo brain samples.
[d]Compound conc. measured in pons/cerebellum samples.

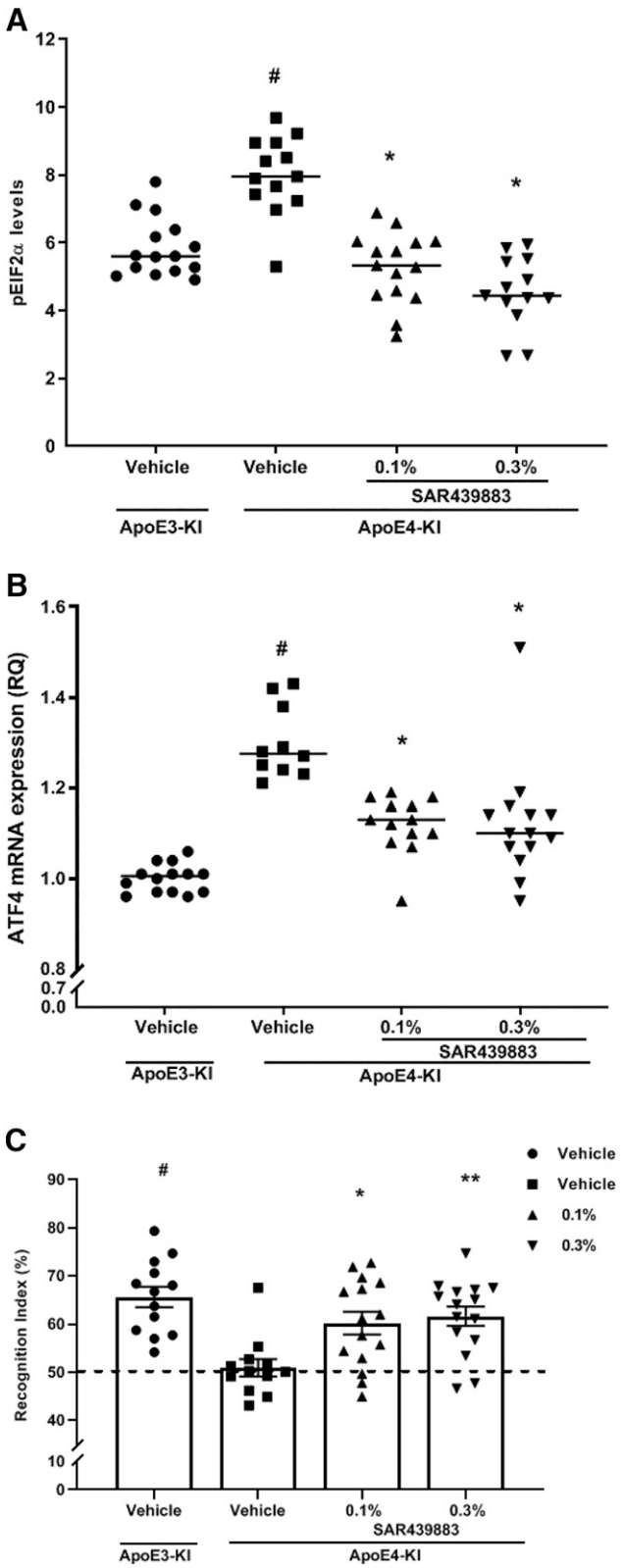

Fig. 2. Effect of subchronic treatment with SAR439883 in ApoE4-KI mice. SAR439883 was administered 7 days in diet. Phosphorylated eIF2 levels, ATF4 mRNA, and short-term memory were evaluated by Western immunoblot and after calculation of phosphorylated eIF2/total eIF2 ratio (A) using real-time PCR (B) and spatial ORT (C), respectively. Data are presented as individual data point from each animal and as means (A and C) and medians (B) from 10 to 15 hippocampus samples per group. Sample size [based on previous experience with these assays (A and C)] and all the analysis steps have been set prior to the experiment. (A) P values are from Dunnett's test versus vehicle groups after a one-way ANOVA, # $P < 0.0001$ versus ApoE3 vehicle; * $P < 0.0001$ versus ApoE4 vehicle. (B) P values are from Dunnett's test after a ranked ΔCT and after one-way ANOVA, # $P < 0.0001$ versus ApoE3 vhicle; * $P < 0.0001$ versus ApoE4 vehicle. (C) P values are from two-way ANOVA on recognition index # $P < 0.0001$ versus ApoE3 vehicle and Dunnett's test after a two-way ANOVA on recognition index *$P = 0.0114$; ** $P = 0.0035$ versus ApoE4 vehicle.

and by 0.3% SAR439883 for the latency parameter ($P = 0.0157$ and $P = 0.0111$, respectively, Fig. 4C), for the number of crossings over the platform, ($P = 0.0201$ and $P = 0.0200$, respectively, Fig. 4D) and for the time spent in target versus opposite quadrant ($P = 0.0153$ and $P = 0.0220$, respectively; Supplemental Fig. 4). AβO's injection did not affect swim speed or total distance. Only mice treated with humanin or with the lower dose of SAR439883 (0.03%) displayed a reduction in both parameters. Swim speed ($P = 0.0286$; $P = 0.0337$) and total distance ($P = 0.0203$; $P = 0.0401$) for humanin and 0.03% of SAR439883-treated mice, respectively, were reduced without affecting the deficit in memory, suggesting that the effects observed on cognition did not reflect dysfunction of locomotion, visual dysfunction, or poor swimming ability.

SAR439883 Prevents Acute AβO-Induced Synapto-Toxicity. At the end of the treatment, brain analysis revealed that protein levels of the postsynaptic marker PSD95 and of the presynaptic markers synaptophysin and SNAP25 were all decreased in AβO-injected mice compared with vehicle mice (Fig. 5A). Hippocampal levels of PSD95 were decreased by 60% (Fig. 5A). Similarly, hippocampal levels of synaptophysin and SNAP25 were decreased by 59% and 44%, respectively (Fig. 5, B and C).

SAR439883 treatment dose-dependently reduced the loss of the three synaptic markers with maximal protection similar to the humanin positive control (Fig. 5).

Brain levels of IL-1β were also shown to be elevated after AβO injection (+251%) and almost fully reversed after treatment with all tested doses of PKR inhibitor (i.e., 82%, 77%, and 91% after 0.03%, 0.1%, and 0.3% in diet, respectively) as well as with humanin treatment (Fig. 5D).

As expected, brain peIF2/eIF2α levels were dose-dependently decreased by SAR439883 treatment (−8%, −16%, and −40% versus vehicle in 0.03%, 0.1%, and 0.3% groups, respectively; Supplemental Fig. 5; Table 3), whereas humanin control did not impact brain peIF2α levels. Notably, AβO injection group had the same levels as vehicle injected. Whole brain kinase occupancy profiling confirmed a dose-dependent and selective binding of SAR439883 to PKR (33%, 65%, 84% for 0.03%, 0.1%, and 0.3% respectively), whereas the other 200 kinases detected were not occupied by the compound (unpublished data; Table 3). Dose-dependent drug exposure in brain was further confirmed (Table 3).

It is noteworthy that, the robust PKR inhibition at the lowest tested dose (0.1% in diet) corresponded to free drug brain concentration of 0.15 μM calculated from values of both unbound fraction in brain and brain exposure (unpublished data; Table 2), consistent with SAR439883 cellular activity.

Discussion

In the present study, we demonstrate that in vivo pharmacological inhibition of the dsRNA activated protein kinase

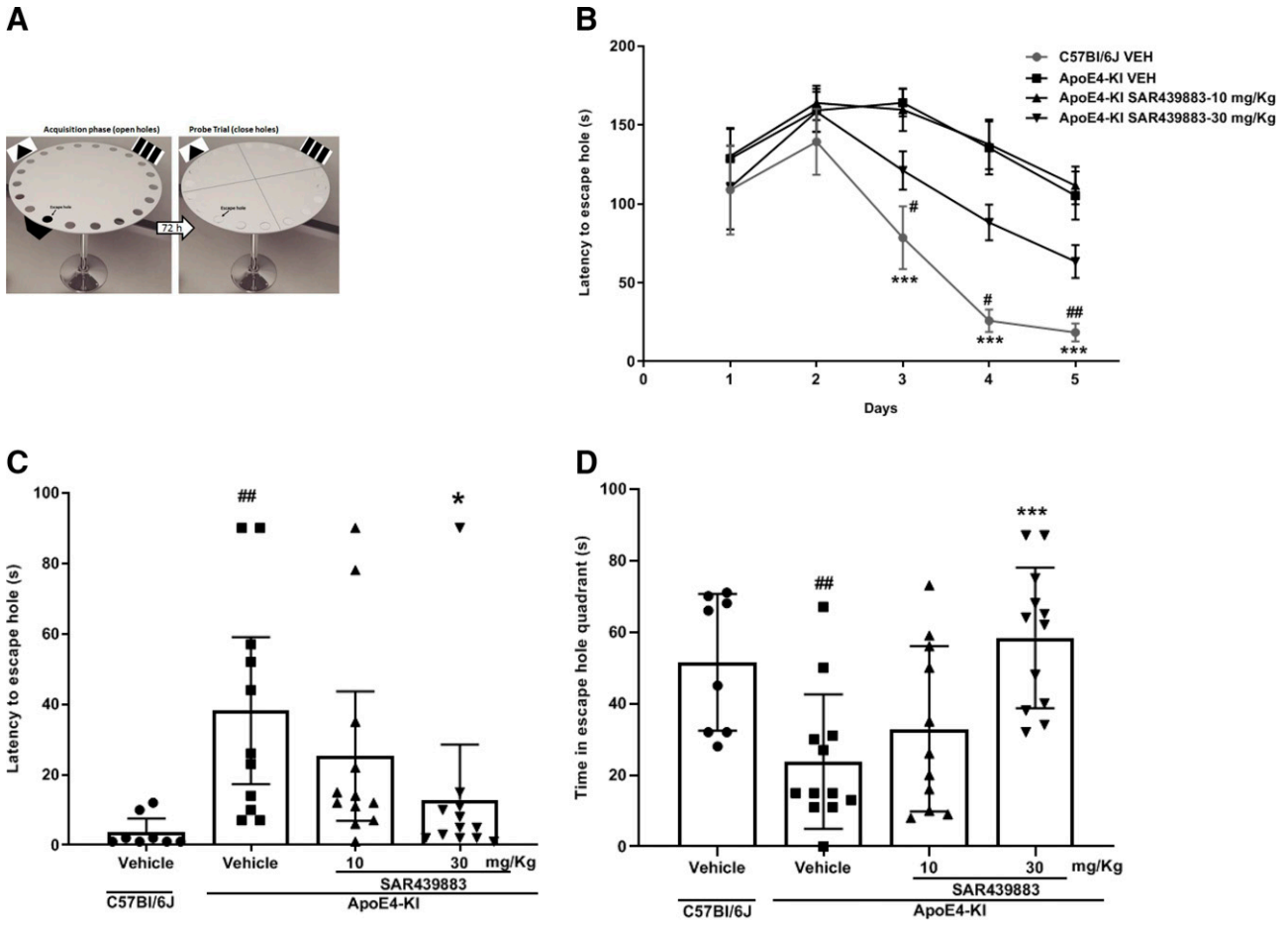

Fig. 3. Effect of subchronic treatment of SAR439883 in learning and long-term memory. SAR439883 was administered by oral route (gavage) at 10 and 30 mg/kg BID for 8 days to ApoE4-KI mice. Spatial learning and long-term memory were assessed using the Barnes Test (A). For latency to the escape hole in the acquisition phase (B), data are presented as medians [Q1; Q3] by group and by day. *P values are obtained from Gehan test at each day between vehicle C57B6/J and vehicle ApoE4-treated mice, ***$P < 0.0003$, $P < 0.0001$ and $P < 0.0001$ for days 3, 4, and 5, respectively. #P values obtained with Gehan tests with Bonferroni-Holm correction of ApoE4-treated mice at 30 mg/kg versus ApoE4 vehicle at each day #$P < 0.0363$, $P < 0.0191$; ##$P < 0.0015$. Probe test was performed 72 hours after the last training day: latency to the escape hole (C) and time in the escape hole quadrant (D). Scatter dot plots show median, [Q1; Q3], maximum and minimum values. #P values are from Student t test ApoE4 vehicle mice versus C57BL6/J for the parameters latency to target hole (C, ## $P = 0.0017$) and time spent in the target zone (D, ## $P = 0.0049$); *P values are obtained from one-way ANOVA followed by a Dunnett's test comparing ApoE4 treated mice versus ApoE4 vehicle mice for the same both parameters (C, *$P = 0.0406$; D, ***$P = 0.0004$). Sample size ($N = 12$) has been calculated after the experiment, as we did not have enough data set.

PKR can decrease cognitive deficits in two relevant experimental models for AD and with synaptoprotective action. SAR439883 is an original isoindolone generated using high-throughput screening and medicinal chemistry optimization. It is highly potent on both murine and human PKR and selective versus the other EIF2AKs PERK, HRI (Heme-regulated eIF2α kinase) , and GCN2 and versus a large panel of kinases and receptors.

Notably, SAR439883 is more potent than the nonselective C16 compound PKR inhibitor largely used in the literature (Ingrand et al., 2007; Chen et al., 2008) and more selective than our previous PKR inhibitor, which was neuroprotective in a thiamine deficiency model (Mouton-Liger et al., 2015). In vivo SAR439883 is orally bioavailable and brain-penetrant and exhibits a safe overall profile.

In line with data by Segev et al. (2013), we confirmed an increase in peIF2α levels (i.e., ratio peIFα/total eIF2α) and of the ATF4 downstream marker in the hippocampus of ApoE4-KI mice. This increase was reversed by our selective PKR inhibitor SAR439883 demonstrating PKR activation in this model. In addition, SAR439883 reversed cognitive deficit in a 7-day treatment, further supporting that inhibition of PKR/peIF2α pathway leads to enhanced long-term memory involving ATF4 reduction in mice as previously suggested (Costa-Mattioli et al., 2007)

Cognitive deficits in ApoE4-KI mice were characterized in the object recognition test (ORT) using experimental conditions close to human clinical tests (Lueptow, 2017), with a 1-hour intertrial interval revealing a deficit in short-term memory as previously reported (Segev et al., 2013). SAR439883 subchronic oral treatment restored short-term memory in ORT as well as learning and long-term memory in the Barnes test in ApoE4-KI mice expanding on findings with the less selective C16 PKR inhibitor (Segev et al., 2015). Interestingly a single administration was not sufficient to restore ORT deficit, suggesting that sustained inhibition is necessary to reverse deficits downstream from peIF2α (unpublished data). Testing SAR439883 in other hippocampus-related behavioral tasks could be useful to

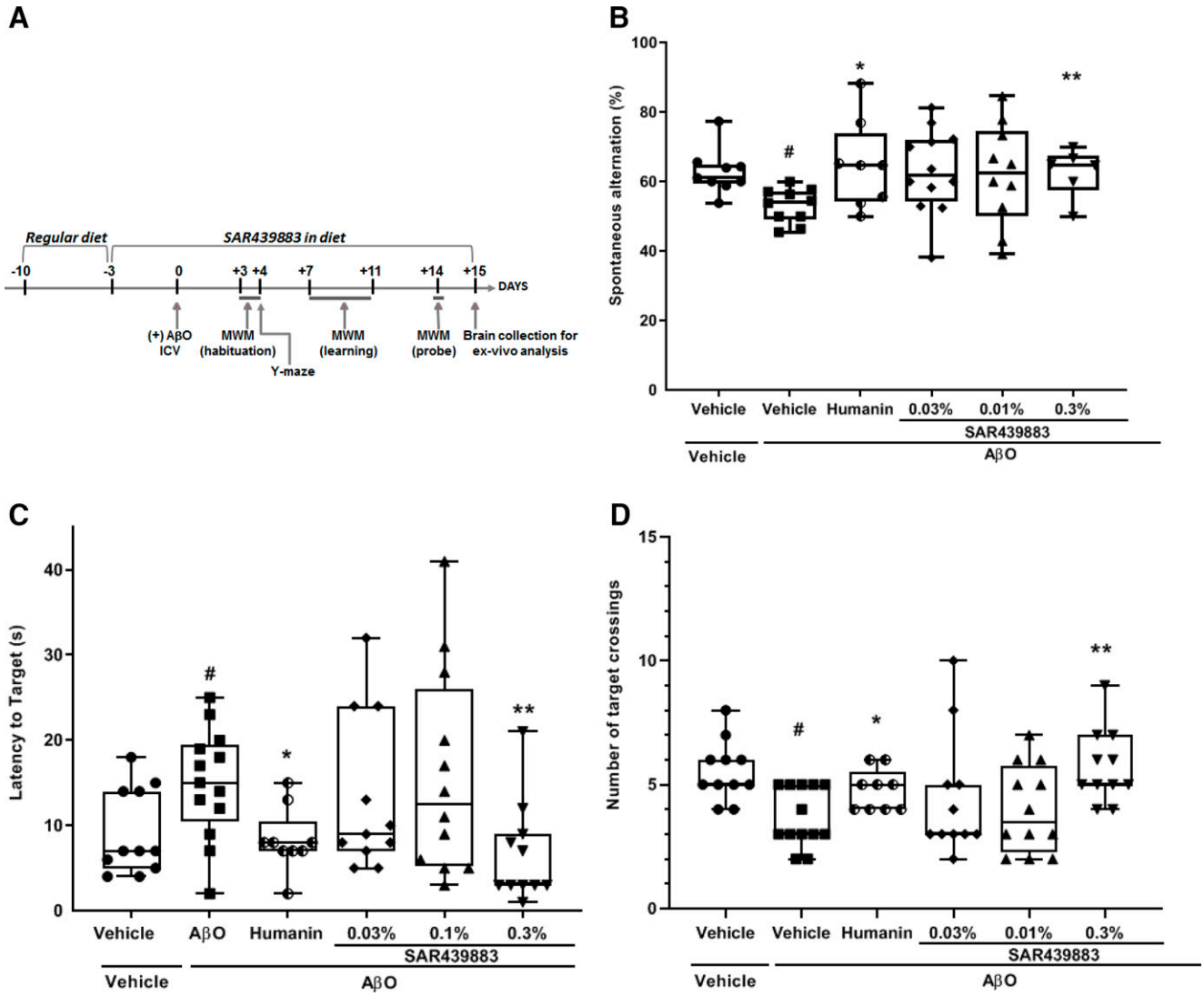

Fig. 4. Effect of SAR439883 on memory impairment in AβO i.c.v. mouse. SAR439883 was administered at 0.03%, 0.1%, and 0.3% in diet for 18 days to AβO i.c.v. injected C57B6/J mice. Schedule of the different tests are described in panel A. The effect on working memory impairment was evaluated using the spontaneous alternation in the Y-maze test (B). *P* values were obtained from either a Student test (vehicle versus AβO; humanin versus AβO) or a one-way ANOVA followed by a Dunnett's test to compare compound effect at 0.03%, 0.1%, and 0.3% in diet to vehicle AβO group. # $P = 0.0019$; * $P = 0.0356$; ** $P = 0.0299$. The effect on spatial long-term memory was evaluated using the MWM (C and D). Individual data and boxplot by group present medians, [Q1; Q3], maximum and minimum values per group and mean ± S.D. Probe test was performed 72 hours after the last training day: latency to target platform. (C) A log-rank test was performed to compare AβO to vehicle group and humanin AβO to AβO group. *P* values are obtained from one-way ANOVA on ranks followed by multiple comparisons with Dunnett's correction. # $P = 0.0338$; * $P = 0.0157$; ** $P = 0.0111$ and number of target crossings. (D) *P* values are from a Student *t* test for pathology induction (AβO versus vehicle) and for humanin effect versus AβO and from Dunnett's test after a one-way ANOVA. # $P = 0.0010$; * $P = 0.0201$; ** $P = 0.0200$. All analysis steps and the sample size per group have been decided before we performed the experiments. Sample size was unequal for one group ($N = 9$) at the beginning of the experiment; $N = 13$ for the rest.

further broaden the spectrum of cognitive functions potentially sensitive to treatment (Segev et al., 2015; Kornecook et al., 2010; Salomon-Zimri et al., 2014). SAR439883 procognitive effect in humanized ApoE4-KI model was associated with highly selective, robust, and dose-dependent inhibition of brain PKR activity. SAR439883 brain-to-plasma ratio is consistently in the range of 0.34, indicating reasonable brain penetration (Hitchcock and Pennington, 2006).

Occupancy of PKR ATP-binding site (using KiNativ technology) was almost complete (90%), demonstrating that PKR was engaged in most cell types in the brain (PKR is largely distributed across brain cell types: endothelial cells and neurons) at the high dose and leading to a 43% inhibition of peIF2α levels. The partial inhibition of peIF2α is consistent with the presence in brain of PERK and GCN2, two other EIF2AKs likely responsible for the residual eIF2α phosphorylation. PERK has been reported to be the major kinase to determine levels of eIF2α phosphorylation in brain (Ounallah-Saad et al., 2014; Gal-Ben-Ari et al., 2019), but, at least in WT and in ApoE4-KI mice, PKR appears to be equally important, accounting for almost half of brain peIF2α levels. We could not generate any reliable data on the levels of phosphorylated PKR due to the mediocre quality of the anti-pPKR antibodies when used with mouse brain tissues.

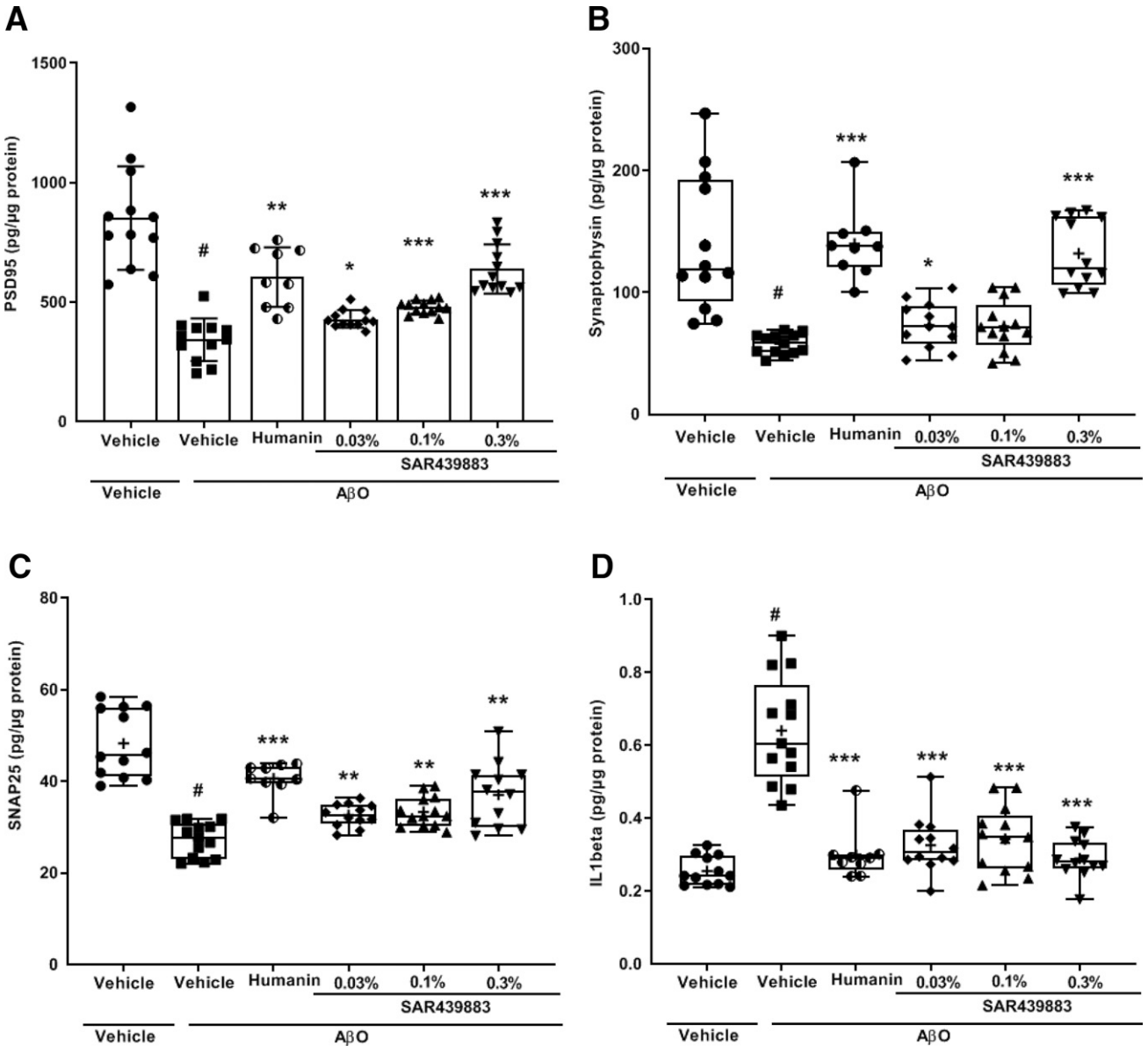

Fig. 5. Effect of SAR439883 18-day diet treatment on synaptic protein loss and inflammation in AβO i.c.v. injection model. SAR439883 was administered at 0.03%, 0.1%, and 0.3% in diet for 18 days to AβO i.c.v. injected mice. At the end of the treatment period, synaptic proteins [i.e., PSD95 (A), synaptophysin (B), SNAP25 (C), and IL-1β (D)] were measured in the individual brain homogenates by ELISA. Individual data and boxplot by group present medians, [Q1; Q3], maximum and minimum values per group, and mean + S.D. *P* values are from Dunnett's test versus AβO after a one-way ANOVA, #$P < 0.0001$ ***$P < 0.0001$, **$P < 0.001$, * $P < 0.05$. All analysis steps and the sample size per group were decided before we performed the experiment. Sample size was unequal for one group ($N = 9$) at the beginning of the experiment; $N = 13$ for the rest.

Remarkably, the ex vivo kinase profiling from brain samples confirmed the potency and selectivity of SAR439883 for PKR among a panel of more than 200 native kinases detected in brain extract. SAR439883 showed minimal interaction with the two EIF2AK GCN2 and PERK, further confirming its in vitro and in-cell high-selectivity profile.

Elevation of phosphorylated eIF2α may also trigger proapoptotic signals through induction of downstream CHOP (Li et al., 2010). However, CHOP was not significantly modulated in ApoE4-KI mice nor after SAR439883 treatment (unpublished data). In addition, we did not observe any modulation of the expression of GADD34, which promotes the dephosphorylation of eIF2α. The absence of modulation of the memory-related transcription factor EGR1 (early growth response 1 factor) suggested that PKR compound could enhance memory via additional ATF4-downstream pathways. Quite similarly, no modulation of downstream markers, such as Trb3 and EBR1 as well as ATF4, is observed in the second experimental model used in this study AβO injection (unpublished data). This could be explained by the rapid and transitory kinetic of this downstream response while it was analyzed during 15-day post–AβO injection.

Our data further underline that partial inhibition of eIF2α via PKR inhibition is sufficient to fully reverse cognitive deficits at least in ApoE4-KI model, consistent with results in eIF2α S51A heterozygote knock-in mice (Costa-Mattioli et al., 2007).

TABLE 3
Effect of an 18-day treatment with SAR439883 on PKR activation and cognition in AβO i.c.v. model

SAR439883 Dose (in Diet; 18 days)	PKR Occupancy in Brain (ActivX/KiNativ™) (%)	peIF2α Inhibition in Brain (% AβO group)	Brain Exposure (μM)
0.03%	**32.7 ± 5.3**[a]	**8.0 ± 0.3** NS	**0.11 ± 0.03**[c]
0.1%	**65.4 ± 7.7**[a]	**15.7 ± 0.5** $P = 0.0096$[b]	**0.34 ± 0.13**[c]
0.3%	**84.2 ± 3.1**[a]	**40.0 ± 1.4** $P < 0.0001$[b]	**1.06 ± 0.34**[c]

[a]Data are from 12 to 13 brain samples (brain cortex) per group that were pooled by 3 to 4 samples.
[b]Data are from 10 to 12 brain samples (hippocampus) per group; *P* values obtained with a Dunnett's test versus AβO after a one-way ANOVA.
[c]Data are from 12 to 13 brain samples (pons/cerebellum) per group.

The intracerebroventricular AβO injection model is considered as a useful complement to transgenic mouse models for the evaluation of therapeutic approaches to AD (Balducci and Forloni, 2014; Ferreira et al., 2015). It recapitulates several features of the disease pathophysiology, including synaptic degeneration without the potential interference of compensation phenomenon linked to the transgenicity from the in-utero stage. Here, we used the acute intracerebroventricular injection of synthetic human Aβ1-42 oligomers rather than $A\beta_{25\text{-}35}$ peptide that has been extensively used but misses the important conformational aspect of the full-length Aβ-derived pathologic species (Murphy and LeVine, 2010).

In accordance with previous reports (Garcia et al., 2010; Ali et al., 2015), a single injection of 50 pmol AβO produced a significant reduction in cognitive performance in Y-maze and MWM after both 4 days (Y-maze) and 15 days (MWM). Both short-term and long-term memory deficits were prevented by SAR439883 treatment consistent with previous studies in PKR-KO mice (Zhu et al., 2011; Lourenco et al., 2013).

In addition, SAR439883 significantly prevented synaptic loss evidenced by the synapse-associated proteins synaptophysin, SNAP25, and PSD95, with similar protection as the neuroprotective humanin reference peptide (Chai et al., 2014).

SAR439883 inhibited the induced production of IL-1β in AβO-injected mice, which would certainly contribute to the overall neuroprotective compound profile. Next steps could include the further documentation of the synapse protective and anti-inflammatory effects of PKR inhibition by immunohistochemistry and using other markers of microglial/astroglial activation that are certainly directly regulated by the eIF2α/ATF4 pathway (Couturier et al., 2012). SAR439883 synaptoprotective effect in vivo is in line with its neuroprotective properties in vitro against AβO and with our previous findings that pharmacologic PKR inhibition can protect against neuronal loss in a thiamine deficiency model characterized by oxidative stress and neuroinflammation (Mouton-Liger et al., 2015). As expected, SAR439883 could robustly decrease brain peIF2α and fully engage its target with high selectivity quite like in the ApoE4-KI model. Previous studies have demonstrated that intracerebroventricular AβO induces peIF2α protein in hypothalamus and hippocampus (Lourenco et al., 2013; Clarke et al., 2015). We failed to detect any significant increase in peIF2α in the present conditions. Potential explanations could be the local increase in peIF2α remained below the detection limit of our analysis on whole hippocampal tissue and the transient nature of peIF2α increase, which we analyzed only 2 weeks after injection. Notably, only a slight increase in peIF2α was observed right after intracerebroventricular AβO injection in a previous study (Hwang et al., 2017).

Interestingly, it has been recently reported that spatial memory, synaptic alteration, and brain inflammation were ameliorated in double-mutant 5xFAD PKR-KO mice at 9 months of age (Tible et al., 2019) and that integrated stress response inhibition, including via PKR deletion could improve behavioral and neurophysiological abnormalities in Down syndrome rodent models (Zhu et al., 2019). We provide here convincing evidence that systemic treatment with a highly selective PKR inhibitor, while leading only to a partial decrease in brain peIF2α levels, prevented AβO-induced synaptic loss, neuroinflammation, and subsequent cognitive deficits and, importantly, could reverse cognitive deficits in ApoE4-KI mice, two animal models highly relevant for AD. Downstream from peIF2α, the ATF4 branch of integrated stress response was downregulated.

These data suggest that PKR could represent a promising target for therapeutic treatment in both sporadic and familial AD.

Acknowledgments:

The authors thank Thierry Pillot (SynAging) for his help with the AbO- intracerebroventricular injection model; Martine Latta-Mahieu (Sanofi) for her help with the project; Albane Courjaud, Irene Mahfouz, Olivier Tempier, Anne Pommeret and Nadine Vaucher (Sanofi) for their help with the biochemical and cellular studies; Bernard Roisil, Joanna Tsi, Celine Prevost, Eric Brohan (Sanofi) for their help with the SAR439883 synthesis; and Laurent Andrieu and his team (Sanofi) for their help with statistical analyses.

Authorship Contributions:

Participated in research design: Lopez-Grancha, Bernardelli, Krick, Sabuco, Machnik, Ibghi, Pradier, Taupin.

Conducted experiments: Lopez-Grancha, Moindrot, Genet, Vincent, Roudieres, Taupin.

Contributed new reagents or analytic tools: Bernardelli, Sabuco, Machnik.

Performed data analysis: Lopez-Grancha, Bernardelli, Krick, Sabuco, Machnik, Ibghi, Taupin.

Wrote or contributed to the writing of the manuscript: Lopez-Grancha, Bernardelli, Ibghi, Pradier, Taupin.

References

Ali T, Yoon GH, Shah SA, Lee HY, and Kim MO (2015) Osmotin attenuates amyloid beta-induced memory impairment, tau phosphorylation and neurodegeneration in the mouse hippocampus. *Sci Rep* **5**:11708.

Badia MC, Lloret A, Giraldo E, Dasí F, Olaso G, Alonso MD, and Viña J (2013) Lymphocytes from young healthy persons carrying the ApoE4 allele overexpress stress-

related proteins involved in the pathophysiology of Alzheimer's disease. *J Alzheimers Dis* **33**:77–83.
Balducci C and Forloni G (2014) In vivo application of beta amyloid oligomers: a simple tool to evaluate mechanisms of action and new therapeutic approaches. *Curr Pharm Des* **20**:2491–2505.
Baleriola J, Walker CA, Jean YY, Crary JF, Troy CM, Nagy PL, and Hengst U (2014) Axonally synthesized ATF4 transmits a neurodegenerative signal across brain regions. *Cell* **158**:1159–1172.
Barnes CA (1979) Memory deficits associated with senescence: a neurophysiological and behavioral study in the rat. *J Comp Physiol Psychol* **93**:74–104.
Bomfim TR, Forny-Germano L, Sathler LB, Brito-Moreira J, Houzel JC, Decker H, Silverman MA, Kazi H, Melo HM, McClean PL, et al. (2012) An anti-diabetes agent protects the mouse brain from defective insulin signaling caused by Alzheimer's disease- associated Aβ oligomers. *J Clin Invest* **122**:1339–1353.
Buffington SA, Huang W, and Costa-Mattioli M (2014) Translational control in synaptic plasticity and cognitive dysfunction. *Annu Rev Neurosci* **37**:17–38.
Chai GS, Duan DX, Ma RH, Shen JY, Li HL, Ma ZW, Luo Y, Wang L, Qi XH, Wang Q, et al. (2014) Humanin attenuates Alzheimer-like cognitive deficits and pathological changes induced by amyloid β-peptide in rats. *Neurosci Bull* **30**:923–935.
Chang RC, Suen KC, Ma CH, Elyaman W, Ng HK, and Hugon J (2002b) Involvement of double-stranded RNA-dependent protein kinase and phosphorylation of eukaryotic initiation factor-2alpha in neuronal degeneration. *J Neurochem* **83**:1215–1225.
Chang RC, Wong AK, Ng HK, and Hugon J (2002a) Phosphorylation of eukaryotic initiation factor-2alpha (eIF2alpha) is associated with neuronal degeneration in Alzheimer's disease. *Neuroreport* **13**:2429–2432.
Chen A, Muzzio IA, Malleret G, Bartsch D, Verbitsky M, Pavlidis P, Yonan AL, Vronskaya S, Grody MB, Cepeda I, et al. (2003) Inducible enhancement of memory storage and synaptic plasticity in transgenic mice expressing an inhibitor of ATF4 (CREB-2) and C/EBP proteins. *Neuron* **39**:655–669.
Chen H-M, Wang L, and D'Mello SR (2008) A chemical compound commonly used to inhibit PKR, 8-(imidazol-4-ylmethylene)-6H-azolidino[5,4-g] benzothiazol-7-one, protects neurons by inhibiting cyclin-dependent kinase. *Eur J Neurosci* **28**:2003–2016.
Clarke JR, Lyra E Silva NM, Figueiredo CP, Frozza RL, Ledo JH, Beckman D, Katashima CK, Razolli D, Carvalho BM, Frazão R, et al. (2015) Alzheimer-associated Aβ oligomers impact the central nervous system to induce peripheral metabolic deregulation. *EMBO Mol Med* **7**:190–210.
Costa-Mattioli M, Gobert D, Stern E, Gamache K, Colina R, Cuello C, Sossin W, Kaufman R, Pelletier J, Rosenblum K, et al. (2007) eIF2alpha phosphorylation bidirectionally regulates the switch from short- to long-term synaptic plasticity and memory. *Cell* **129**:195–206.
Costa-Mattioli M, Sossin WS, Klann E, and Sonenberg N (2009) Translational control of long-lasting synaptic plasticity and memory. *Neuron* **61**:10–26.
Couturier J, Paccalin M, Lafay-Chebassier C, Chalon S, Ingrand I, Pinguet J, Pontcharraud R, Guillard O, Fauconneau B, and Page G (2012) Pharmacological inhibition of PKR in APPswePS1dE9 mice transiently prevents inflammation at 12 months of age but increases Aβ42 levels in the late stages of the Alzheimer's disease. *Curr Alzheimer Res* **9**:344–360.
Delay-Goyet P, Blanchard V, Schussler N, Lopez-Grancha M, Ménager J, Mary V, Sultan E, Buzy A, Guillemot JC, Stemmelin J, et al. (2016) SAR110894, a potent histamine H3-receptor antagonist, displays disease-modifying activity in a transgenic mouse model of tauopathy. *Alzheimers Dement (N Y)* **2**:267–280 NY.
Dumurgier J, Mouton-Liger F, Lapalus P, Prevot M, Laplanche JL, Hugon J, and Paquet C; Groupe d'Investigation du Liquide Cephalorachidien (GIL) Study Network (2013) Cerebrospinal fluid PKR level predicts cognitive decline in Alzheimer's disease. *PLoS One* **8**:e53587.
Ennaceur A and Delacour J (1988) A new one-trial test for neurobiological studies of memory in rats. 1: Behavioral data. *Behav Brain Res* **31**:47–59.
Ferreira ST and Klein WL (2011) The Aβ oligomer hypothesis for synapse failure and memory loss in Alzheimer's disease. *Neurobiol Learn Mem* **96**:529–543.
Ferreira ST, Lourenco MV, Oliveira MM, and De Felice FG (2015) Soluble amyloid-β oligomers as synaptotoxins leading to cognitive impairment in Alzheimer's disease. *Front Cell Neurosci* **9**:191.
Gal-Ben-Ari S, Barrera I, Ehrlich M, and Rosenblum K (2019) PKR: a kinase to remember. *Front Mol Neurosci* **11**:480.
Garcia P, Youssef I, Utvik JK, Florent-Béchard S, Barthélémy V, Malaplate-Armand C, Kriem B, Stenger C, Koziel V, Olivier JL, et al. (2010) Ciliary neurotrophic factor cell-based delivery prevents synaptic impairment and improves memory in mouse models of Alzheimer's disease. *J Neurosci* **30**:7516–7527.
Harding HP, Zeng H, Zhang Y, Jungries R, Chung P, Plesken H, Sabatini DD, and Ron D (2001) Diabetes mellitus and exocrine pancreatic dysfunction in perk-/- mice reveals a role for translational control in secretory cell survival. *Mol Cell* **7**:1153–1163.
Hitchcock SA and Pennington LD (2006) Structure-brain exposure relationships. *J Med Chem* **49**:7559–7583.
Hughes RN (2004) The value of spontaneous alternation behavior (SAB) as a test of retention in pharmacological investigations of memory. *Neurosci Biobehav Rev* **28**:497–505.
Hugon J, Mouton-Liger F, Dumurgier J, and Paquet C (2017) PKR involvement in Alzheimer's disease. *Alzheimers Res Ther* **9**:83.
Hwang KD, Bak MS, Kim SJ, Rhee S, and Lee YS (2017) Restoring synaptic plasticity and memory in mouse models of Alzheimer's disease by PKR inhibition. *Mol Brain* **10**:57.
Ingrand S, Barrier L, Lafay-Chebassier C, Fauconneau B, Page G, and Hugon J (2007) The oxindole/imidazole derivative C16 reduces in vivo brain PKR activation. *FEBS Lett* **581**:4473–4478.
Kim J, Basak JM, and Holtzman DM (2009) The role of apolipoprotein E in Alzheimer's disease. *Neuron* **63**:287–303.
Kornecook TJ, McKinney AP, Ferguson MT, and Dodart JC (2010) Isoform-specific effects of apolipoprotein E on cognitive performance in targeted-replacement mice overexpressing human APP. *Genes Brain Behav* **9**:182–192.
Li G, Scull C, Ozcan L, and Tabas I (2010) NADPH oxidase links endoplasmic reticulum stress, oxidative stress, and PKR activation to induce apoptosis. *J Cell Biol* **191**:1113–1125.
Lourenco MV, Clarke JR, Frozza RL, Bomfim TR, Forny-Germano L, Batista AF, Sathler LB, Brito-Moreira J, Amaral OB, Silva CA, et al. (2013) TNF-α mediates PKR-dependent memory impairment and brain IRS-1 inhibition induced by Alzheimer's β-amyloid oligomers in mice and monkeys. *Cell Metab* **18**:831–843.
Lu PD, Harding HP, and Ron D (2004) Translation reinitiation at alternative open reading frames regulates gene expression in an integrated stress response. *J Cell Biol* **167**:27–33.
Lueptow LM (2017) Novel object recognition test for the investigation of learning and memory in mice. *J Vis Exp* **126**:55718.
Ma T, Trinh MA, Wexler AJ, Bourbon C, Gatti E, Pierre P, Cavener DR, and Klann E (2013) Suppression of eIF2α kinases alleviates Alzheimer's disease-related plasticity and memory deficits. *Nat Neurosci* **16**:1299–1305.
Mamada N, Tanokashira D, Hosaka A, Kametani F, Tamaoka A, and Araki W (2015) Amyloid β-protein oligomers upregulate the β-secretase, BACE1, through a post-translational mechanism involving its altered subcellular distribution in neurons. *Mol Brain* **8**:73.
Means LW, Leander JD, and Isaacson RL (1971) The effects of hippocampectomy on alternation behavior and response of novelty. *Physiol Behav* **6**:17–22.
Meziane H, Ouagazzal AM, Aubert L, Wietrzych M, and Krezel W (2007) Estrous cycle effects on behavior of C57BL/6J and BALB/cByJ female mice: implications for phenotyping strategies. *Genes Brain Behav* **6**:192–200.
Morel M, Couturier J, Lafay-Chebassier C, Paccalin M, and Page G (2009) PKR, the double stranded RNA-dependent protein kinase as a critical target in Alzheimer's disease. *J Cell Mol Med* **13** (8A):1476–1488.
Mouton-Liger F, Paquet C, Dumurgier J, Lapalus P, Gray F, Laplanche JL, and Hugon J; Groupe d'Investigation du Liquide Céphalorachidien Study Network (2012) Increased cerebrospinal fluid levels of double-stranded RNA-dependant protein kinase in Alzheimer's disease. *Biol Psychiatry* **71**:829–835.
Mouton-Liger F, Rebillat AS, Gourmaud S, Paquet C, Leguen A, Dumurgier J, Bernadelli P, Taupin V, Pradier L, Rooney T, et al. (2015) PKR downregulation prevents neurodegeneration and β-amyloid production in a thiamine-deficient model. *Cell Death Dis* **6**:e1594.
Murphy MP and LeVine 3rd H (2010) Alzheimer's disease and the amyloid-beta peptide. *J Alzheimers Dis* **19**:311–323.
Onuki R, Bando Y, Suyama E, Katayama T, Kawasaki H, Baba T, Tohyama M, and Taira K (2004) An RNA-dependent protein kinase is involved in tunicamycin-induced apoptosis and Alzheimer's disease. *EMBO J* **23**:959–968.
Ounallah-Saad H, Sharma V, Edry E, and Rosenblum K (2014) Genetic or pharmacological reduction of PERK enhances cortical-dependent taste learning. *J Neurosci* **34**:14624–14632.
Paccalin M, Pain-Barc S, Pluchon C, Paul C, Besson MN, Carret-Rebillat AS, Rioux-Bilan A, Gil R, and Hugon J (2006) Activated mTOR and PKR kinases in lymphocytes correlate with memory and cognitive decline in Alzheimer's disease. *Dement Geriatr Cogn Disord* **22**:320–326.
Page G, Rioux Bilan A, Ingrand S, Lafay-Chebassier C, Pain S, Perault Pochat MC, Bouras C, Bayer T, and Hugon J (2006) Activated double-stranded RNA-dependent protein kinase and neuronal death in models of Alzheimer's disease. *Neuroscience* **139**:1343–1354.
Paquet C, Dumurgier J, and Hugon J (2015) Pro-apoptotic kinase levels in cerebrospinal fluid as potential future biomarkers in Alzheimer's disease. *Front Neurol* **6**:168.
Paquet C, Mouton-Liger F, Meurs EF, Mazot P, Bouras C, Pradier L, Gray F, and Hugon J (2012) The PKR activator PACT is induced by Aβ: involvement in Alzheimer's disease. *Brain Pathol* **22**:219–229.
Peel AL and Bredesen DE (2003) Activation of the cell stress kinase PKR in Alzheimer's disease and human amyloid precursor protein transgenic mice. *Neurobiol Dis* **14**:52–62.
Roberts WW, Dember WN, and Brodwick M (1962) Alternation and exploration in rats with hippocampal lesions. *J Comp Physiol Psychol* **55**:695–700.
Salomon-Zimri S, Boehm-Cagan A, Liraz O, and Michaelson DM (2014) Hippocampus-related cognitive impairments in young apoE4 targeted replacement mice. *Neurodegener Dis* **13**:86–92.
Segev Y, Michaelson DM, and Rosenblum K (2013) ApoE ε4 is associated with eIF2α phosphorylation and impaired learning in young mice. *Neurobiol Aging* **34**:863–872.
Segev Y, Barrera I, Ounallah-Saad H, Wibrand K, Sporild I, Livne A, Rosenberg T, David O, Mints M, Bramham CR, et al. (2015) PKR inhibition rescues memory deficit and ATF4 overexpression in ApoE ε4 human replacement mice. *J Neurosci* **35**:12986–12993.
Stern E, Chinnakkaruppan A, David O, Sonenberg N, and Rosenblum K (2013) Blocking the eIF2α kinase (PKR) enhances positive and negative forms of cortex-dependent taste memory. *J Neurosci* **33**:2517–2525.
Sullivan PM, Mezdour H, Aratani Y, Knouff C, Najib J, Reddick RL, Quarfordt SH, and Maeda N (1997) Targeted replacement of the mouse apolipoprotein E gene with the common human APOE3 allele enhances diet-induced hypercholesterolemia and atherosclerosis. *J Biol Chem* **272**:17972–17980.
Tible M, Mouton Liger F, Schmitt J, Giralt A, Farid K, Thomasseau S, Gourmaud S, Paquet C, Rondi Reig L, Meurs E, et al. (2019) PKR knockout in the 5xFAD model of Alzheimer's disease reveals beneficial effects on spatial memory and brain lesions. *Aging Cell* **18**:e12887.
Vattem KM and Wek RC (2004) Reinitiation involving upstream ORFs regulates ATF4 mRNA translation in mammalian cells. *Proc Natl Acad Sci USA* **101**:11269–11274.

Viola KL and Klein WL (2015) Amyloid β oligomers in Alzheimer's disease pathogenesis, treatment, and diagnosis. *Acta Neuropathol* **129**:183–206.
Yuan L, Liu XJ, Han WN, Li QS, Wang ZJ, Wu MN, Yang W, and Qi JS (2016) [Gly14]-Humanin protects against amyloid β peptide-induced impairment of spatial learning and memory in rats. *Neurosci Bull* **32**:374–382.
Zhu PJ, Huang W, Kalikulov D, Yoo JW, Placzek AN, Stoica L, Zhou H, Bell JC, Friedlander MJ, Krnjević K, et al. (2011) Suppression of PKR promotes network excitability and enhanced cognition by interferon-γ-mediated disinhibition. *Cell* **147**:1384–1396.
Zhu PJ, Khatiwada S, Cui Y, Reineke LC, Dooling SW, Kim JJ, Li W, Walter P, and Costa-Mattioli M (2019) Activation of the ISR mediates the behavioral and neurophysiological abnormalities in Down syndrome. *Science* **366**:843–849.
Zhu S, Henninger K, McGrath BC, and Cavener DR (2016) PERK regulates working memory and protein synthesis-dependent memory flexibility. *PLoS One* **11**:e0162766.

Address correspondence to: Dr. Veronique Taupin, Sanofi R&D, 371 Av Prof. Blayac, 34184 Montpellier, France. E-mail: veronique.taupin@sanofi.com